metals

MDPI

Article

Joining of Zirconia to Ti6Al4V Using Ag-Cu Sputter-Coated Ti Brazing Filler

Sónia Simões [1,2,*], Omid Emadinia [2], Carlos José Tavares [3] and Aníbal Guedes [4,5]

[1] Department of Metallurgical and Materials Engineering, University of Porto, Rua Dr. Roberto Frias, 4200-465 Porto, Portugal
[2] LAETA/INEGI-Institute of Science and Innovation in Mechanical and Industrial Engineering, Rua. Dr. Roberto Frias, 4200-465 Porto, Portugal; oemadinia@inegi.up.pt
[3] Physics Centre of the Universities of Minho and Porto (CF-UM-PT), Campus of Azurém, 4804-533 Guimarães, Portugal; ctavares@fisica.uminho.pt
[4] Department of Mechanical Engineering, CMEMS-UMinho, University of Minho, Azurém, 4800-058 Guimarães, Portugal; aguedes@dem.uminho.pt
[5] LABBELS–Associate Laboratory, Braga, 4800-058 Guimarães, Portugal
* Correspondence: ssimoes@fe.up.pt; Tel.: +351-22041-3113

Abstract: The joining of zirconia (ZrO_2) to Ti6Al4V using Ag-Cu sputter-coated Ti brazing filler foil was investigated. Brazing experiments were performed at 900, 950, and 980 °C for 30 min under vacuum. The microstructural features of the brazed interfaces were evaluated by optical microscopy (OM) and by scanning electron microscopy (SEM). The chemical composition of the brazed interfaces was analyzed by energy dispersive X-ray spectroscopy (EDS). Room temperature shear tests and Vickers microhardness tests performed across the interfaces were used to evaluate the mechanical strength of the joints. Multilayered interfaces were produced for all brazing temperatures, consisting essentially in α-Ti + Ti_2(Ag, Cu), TiAg. Joining to ZrO_2 was promoted by the formation of a hard layer, reaching a maximum of 1715 HV0.01, possibly consisting mainly in α-Ti and Ti oxide(s). Joining to the Ti6Al4V was established by a layer composed of a mixture of α-Ti and Ti_2(Ag, Cu). The highest shear strength (152 ± 4 MPa) was obtained for brazing at 980 °C and fracture of joints occurred partially across the interface, throughout the hardest layers formed close to ZrO_2, and partially across the ceramic sample.

Keywords: zirconia; Ti6Al4V; brazing; interface; microstructure; microhardness; shear strength; sputtering

Citation: Simões, S.; Emadinia, O.; Tavares, C.J.; Guedes, A. Joining of Zirconia to Ti6Al4V Using Ag-Cu Sputter-Coated Ti Brazing Filler. *Metals* **2022**, *12*, 358. https://doi.org/10.3390/met12020358

Academic Editor: Marcello Cabibbo

Received: 5 February 2022
Accepted: 18 February 2022
Published: 20 February 2022

1. Introduction

Ti6Al4V alloy, due to its excellent performance and attractive properties, such as high-temperature specific strength, low density, excellent creep, and corrosion resistance, is the most used commercial titanium alloy [1]. Combining this titanium alloy with advanced ceramics, e.g., zirconia (ZrO_2) or alumina (Al_2O_3), which have high wear resistance, excellent thermal stability, or even thermal and electrical conductivity, can be interesting for applications in electronics, aerospace, nuclear and transportation industries [2,3]. However, the production of complex-shaped and large-sized components is complex due to the inherent brittleness of ceramics [3]. The possibility of joining ceramic materials to metals can be an excellent option to overcome the challenges in producing this component.

For ceramic-metal joining, diffusion bonding and brazing are the most reported processes that produce a homogeneous interface and high strength joints [4]. Brazing using Ti-based or Ag-based filler alloys or even amorphous fillers is an auspicious processing route to produce dissimilar ZrO_2 and Ti6Al4V joints [5–13]. Ag-based fillers seem to be a suitable option to overcome the problems related to poor wettability and the development of residual stresses at the brazing interface. The use of these alloys requires low brazing temperatures (from 860 to 880 °C), however the shear strength of joints is reported to be

as low as 52 MPa [5]. The formation of (Ag) at the interface is rarely avoided, which is detrimental to the allowable service temperature of joints [14]. Other brittle intermetallic compounds are generally present at the interface, such as Ti-Cu-Al. Brazing with Ti-based filler alloys allows producing joints with higher shear strength (c.a. 113 MPa) [6]. However, higher brazing temperatures are required. The brazing temperature can be a critical issue for joining Ti6Al4V since they often exceed the β-transus of this alloy, as temperatures around or above 1000 °C are typically needed.

There are several possibilities for improving the mechanical properties of these dissimilar joints. Alloying the braze with active/reactive elements, such as Ti, to enhance the formation of phases that are chemically compatible with both the ceramic and metallic parts of the joining is a common practice. Furthermore, other alloying additions could promote the formation of more favorable phases at the interface. Another option consists of brazing with alloys designed to improve diffusion during the bonding process. For instance, Dai et al. [7] investigated the effect of WB addition on the Ag-28Cu (wt%) filler alloy for brazing Ti6Al4V to ZrO_2. The addition of 7.5 wt% of WB promoted of joints with a shear strength of 83 MPa after processing at 870 °C. The addition of WD particles to the brazing alloy proved to be effective in relieving residual stresses, leading to the improved mechanical performance of the joints.

The use of amorphous filler alloys can also be an appropriate approach for brazing titanium alloys to ZrO_2, as shown by Liu et al. [8,9]. These authors studied the joining of Ti6Al4V to ZrO_2 using Ti-based amorphous filler. Brazing was performed at temperatures between 850 and 1000 °C using Ti-28Zr-14Cu-11Ni foil. The processing temperature had a significant impact on the possibility of producing defect-free interfaces. The maximum shear strength was obtained for joints processed at 850 °C for 30 min (63 MPa). In another work [11], Ti-17Zr-50Cu amorphous brazing filler was used, and the highest shear strength (162 MPa) was obtained for joints processed at 900 °C for 10 min. Higher mechanical strength for Ti6Al4V/ZrO_2 joints was reported by Cao et al. [12]. In this study, a NiCrSiB amorphous foil was used as a brazing filler for joining at temperatures ranging from 950 to 1050 °C, with a dwelling stage of 10 min and an applied pressure of 30 kPa. Although defect-free interfaces were produced with a shear strength of 160 MPa at 950 °C, the highest shear strength (284 MPa) value was obtained for joints processed at 1025 °C.

In previous works [15–17], a Ti foil sputter-coated with Ag and Cu films was successfully used as filler to braze several materials systems. Specifically, this brazing filler was used to produce Al_2O_3/γ-TiAl alloy and Al_2O_3/Ti6Al4V joints [15], as well as γ-TiAl alloy/Hastelloy [16] and similar γ-TiAl alloy joints [17]. In all these studies, the large formation amount of (Ag) at the interface was avoided, potentially enhancing the operating temperature of joints. In addition, the extensive formation of hard phases was also pre-vented, and consequently, the need to perform post-brazing heat treatments was avoided [14]. The reported results were promising for the prospective use of this filler for brazing other systems of dissimilar materials, for joining ceramics to metals.

In this context, the present study aims to evaluate the use of this novel Ag-Cu sputter-coated Ti brazing filler to join ZrO_2 to Ti6Al4V alloy. The interfacial microstructural and chemical features of the brazed interfaces were analyzed by scanning electron microscopy and energy dispersive X-ray spectroscopy. Vickers microhardness and room temperature shear tests were used to evaluate the mechanical strength of joints.

2. Materials and Methods

The production conditions and the microstructural characterization of the Ag-Cu sputter-coated Ti brazing filler were previously described [15,16]. The filler is composed of a Ti foil coated on both sides with an Ag film (20 μm) followed by a Cu film (5 μm); the total thickness of the filler is 150 μm. ZrO_2 stabilized with magnesia and a Ti6Al4V (α-β) alloy sample were wet grounded with SiC paper to a 1200 mesh finish, then degreased in acetone with ultrasonic agitation and dried in air. Samples for brazing were assembled into sandwich-type, with the brazing filler inserted in the middle, using a stainless steel fixing

feature. Brazing experiments were performed at 900, 950, and 980 °C for 30 min in vacuum (better than 10^{-4} mbar) with heating and cooling rates set to 5 °C/min. This set of brazing temperatures was selected based on the better results achieved in previous works using the same brazing filler alloy [15–17].

Joints for microstructural characterization were prepared using conventional metallographic techniques. The microstructure of the interfaces was characterized by OM, using DM4000 equipment (Leica Microsystems, Wetzlar, Germany) and by SEM using a Thermo Fisher Scientific QUANTA 400 FEG equipment (Thermo Fisher Scientific, Hillsboro, OR, USA). SEM and EDS (EDAX Genesis X4M, EDAX Inc. (Ametek), Mahwah, NJ, USA) analyses were performed at an accelerating voltage of 15 keV for mapping and local analysis using the standardless quantification method. All chemical compositions will be expressed in at.%.

The mechanical behavior of brazed interfaces was assessed by Vickers microhardness measurements on the polished interfaces and the mechanical strength of joints was evaluated by room temperature shear tests. Vickers microhardness tests were performed with a 98-mN load (HV0.01) using Duramin-1 Struers equipment (Duramin-1; Struers A/S, Ballerup, Denmark). The hardness maps were obtained by indentation matrices up to 4 rows per 27 columns. The scheme of the matrices across the interface is represented in Figure 1. The shear tests were performed in a universal testing machine, with a crosshead speed of 0.2 mm/min, using the apparatus presented in Figure 2. For each brazing temperature, four joints were shear tested. The fracture surfaces of shear tested joints were observed using a digital microscope DVM6 (Leica Microsystems, Wetzlar, Germany) and analyzed by SEM/EDS.

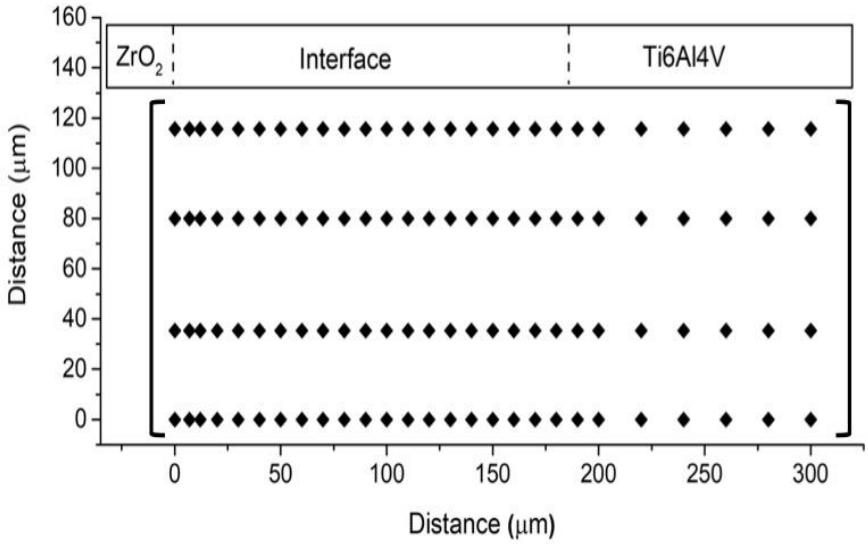

Figure 1. The matrix for the Vickers microhardness test showing the indentation position (♦) across the joint interface.

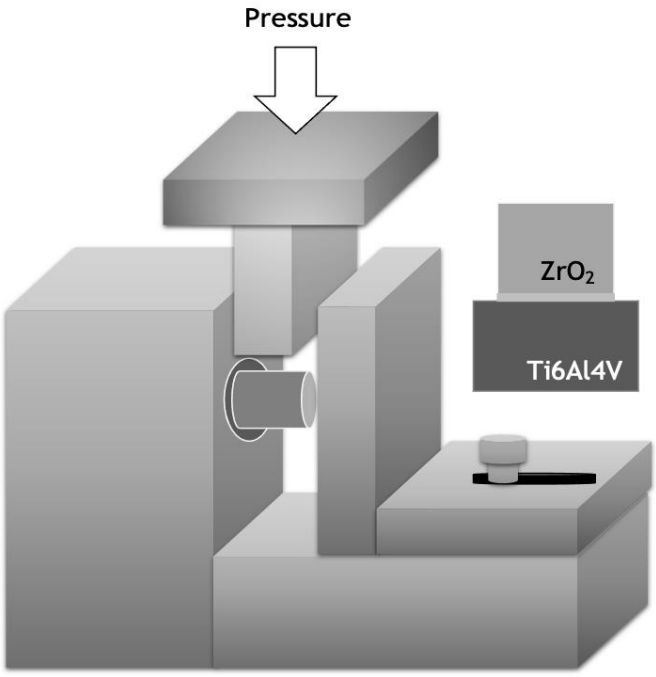

Figure 2. Schematic illustration of the shear strength test apparatus used.

3. Results

The interfacial microstructural of joints is rather complex and strongly influenced by the brazing temperature. Figure 3 shows SEM images of the interfaces of the joints processed at 900, 950, and 980 °C. The interface could be divided into up to five layers and at 900 °C, starting from the base ZrO_2 sample, it could be described as the following sequence of layers: (i) a layer consisting in a mixture of dark zones with bright smaller particles mainly located at its center (layer **1**); (ii) a layer, with a rather irregular thickness that consists of two sub-layers (layer **2**), one essentially consisting in a light grey phase, followed by another composed of grey phase that delimits this layer from layer **3**; (iii) the central region of the interface, composed of a mixture coarse grey plates and lamellar zones (layer 3); (iv) a layer presenting the same microstructural features as layer **2** (layer **4**); (v) a layer presenting some similar microstructural features to those of the central region of the interface and another similar to those of the base Ti6Al4V alloy (layer **5**).

Increasing the brazing temperature to 950 °C increases the thickness of layer **1** and eliminates most of the bright particles that were observed dispersed in this layer after brazing at 900 °C. The pores (red arrows marked in Figure 3) observed for all brazing temperatures are a noteworthy feature of layer **1**. After brazing at 900 °C, porosity is detected in the vicinity of the base ZrO_2 sample, while after brazing at 980 °C porosity it is essential it is observed close to layer **2**. The worst porosity feature is observed after brazing at 950 °C, since pores are observed near the ZrO_2 sample as well as close to layer **2**.

The interfaces obtained at 950 and 980 °C are somewhat similar, differing in thickness and in a few microstructural features presented by some of the layers. For instance, the thickness of layer **2**, although rather irregular, tends to increase as the brazing temperature increases and for the higher processing temperatures this layer is mainly composed of the grey phase that was delimiting the central zone of interface after brazing at 900 °C. The thickness of layer **3**, which corresponds to c.a. 50% of the overall thickness of the interface, decreases as the brazing temperature is incremented and its microstructure tends to coarsen. Layer **4** is barely observable after joining at 980 °C and consists of a mixture of light grey particles and lamellar zones that are similar to those observed in layer **3**, although with coarser lamellae. Finally, the thickness of layer **5** tends to increase as the processing temperature is incremented.

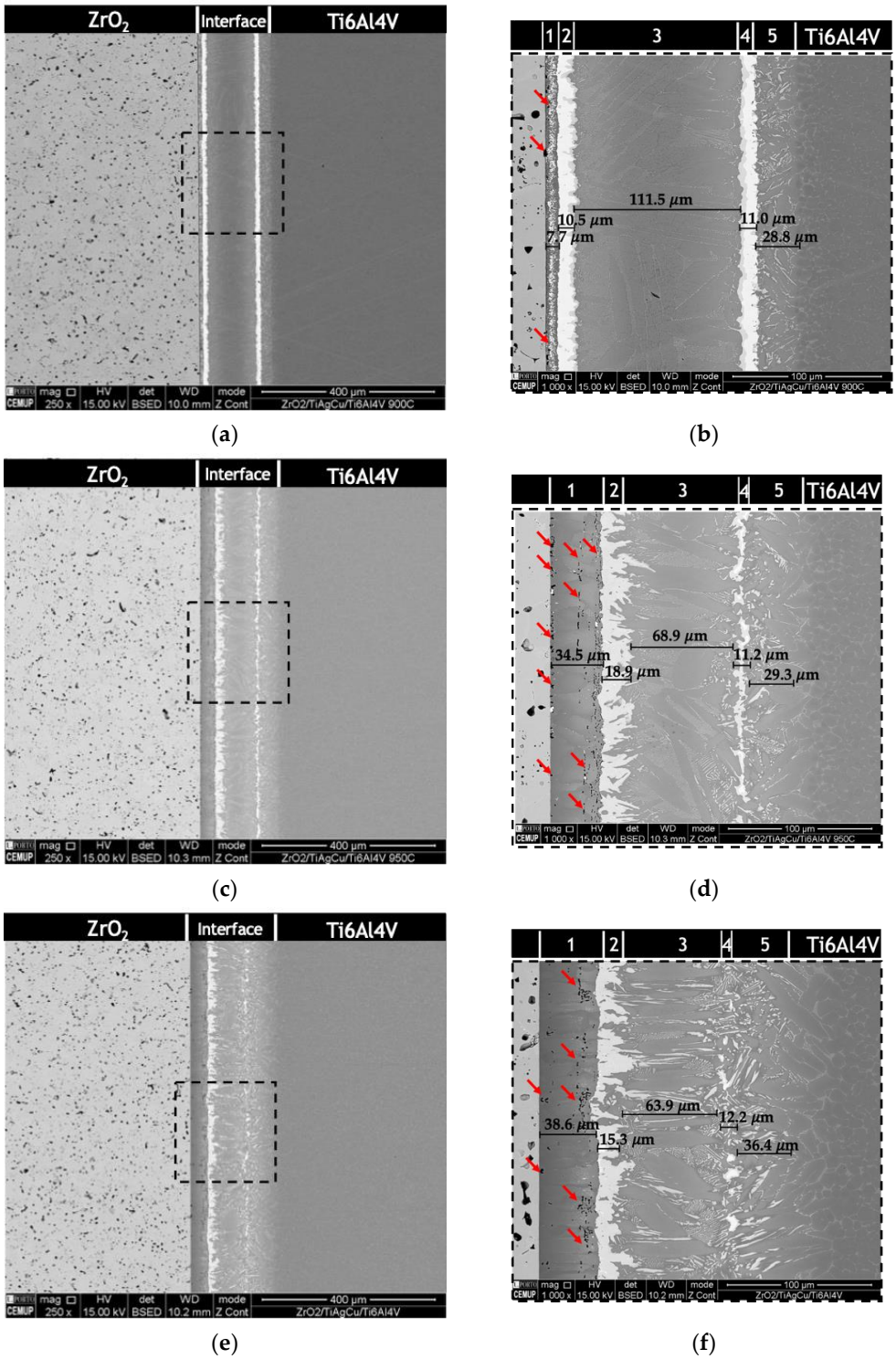

(**a**) (**b**)

(**c**) (**d**)

(**e**) (**f**)

Figure 3. SEM images of the of ZrO_2/Ti6Al4V alloy brazed interfaces processed at: (**a**,**b**) 900 °C, (**c**,**d**) 950 °C and (**e**,**f**) 980 °C.

A SEM image of the interface and EDS interfacial elemental distribution maps of ZrO_2/Ti6Al4V joints processed at 980 °C are presented in Figure 4. The distribution map of oxygen shows that this element is detected at the interface only in layer **1**, close to the ceramic sample and in low contents, indicating the eventual formation of a thin oxide sub-layer. Ag, Cu and Ti are present throughout the entire interface, although Ag is mainly

detected in layers **2** and **4**, in contrast to Ti, which is the element detected in higher contents across the interface.

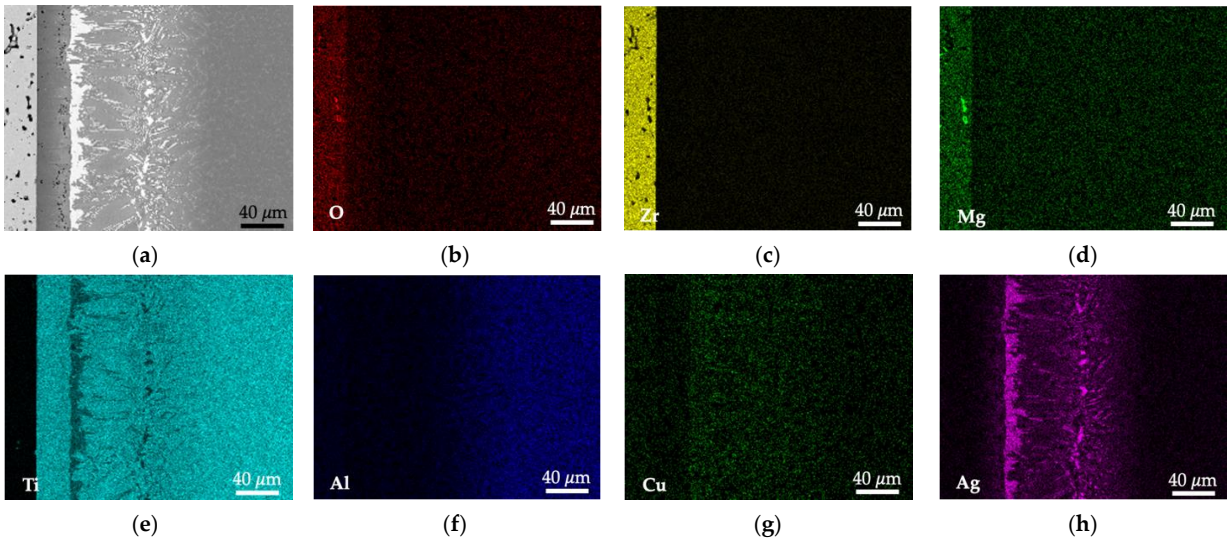

Figure 4. (**a**) SEM image and (EDS) elemental distribution maps of (**b**) O, (**c**) Zr, (**d**), Mg (**e**) Ti, (**f**) Al, (**g**) Cu and (**h**) Ag of the brazed interface of ZrO_2/Ti6Al4V joint processed at 980 °C.

To identify the possible phases constituting the reaction layers formed at the interfaces, EDS chemical analyses results and SEM images of the interfaces were combined with the information provided by the Ti-Al [18], Ti-Al-Ag [19,20], Ti-Ag-Cu [19], Ti-Al-V [21], Ti-Al-Nb [22] and Ti-Al-Cu [23] equilibrium phase diagrams. Figure 5 presents SEM images of the interfaces showing typical detailed microstructural features for the three brazing temperatures. The EDS analysis results of each zone marked in these images are shown in Table 1.

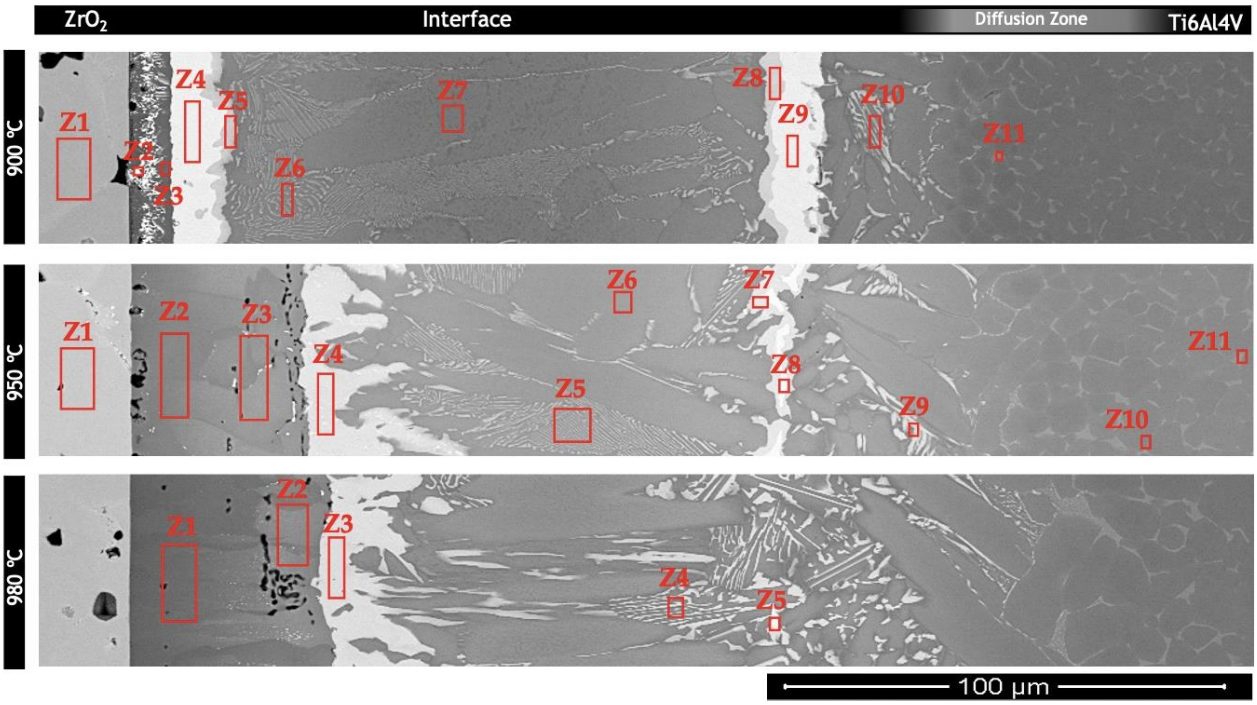

Figure 5. SEM images of ZrO_2/Ti6Al4V alloy interfaces obtained at 900, 950, and 980 °C with indication of the EDS analyzed zones.

Table 1. EDS chemical composition (at.%) of the zones of interest is illustrated in Figure 5.

Zone		Ag	Ti	Cu	Zr	Mg	O	Al	V	Possible Main Phase (s)
900 °C	1				38.3	4.6	57.0			ZrO_2
	2	95.8	4.2							(Ag)
	3	2.2	97.8	-						α-Ti
	4	51.8	48.2	-	-	-	-			TiAg
	5	28.7	64.3	7	-	-	-			Ti_2(Cu, Ag)
	6	4.3	89.8	5.9						α-Ti + Ti_2(Cu, Ag)
	7	-	98.6	1.4						α-Ti
	8	31.2	64.0	4.8						Ti_2(Cu, Ag)
	9	50.9	49.1							TiAg
	10	4.5	77.5	5.7				6.3	5.9	α-Ti + Ti_2(Cu, Ag)
	11	-	88.3	-				10.6	1.2	α-Ti
950 °C	1				39.2	4.3	56.5			ZrO_2
	2	1.7	98.3							α-Ti
	3	4.2	95.8							α-Ti
	4	19.8	75.6	4.6						Ti_2(Cu, Ag)
	5	5.0	88.6	6.4						α-Ti + Ti_2(Cu, Ag)
	6	2.6	95.8	1.6						α-Ti
	7	31.8	65	3.2						TiAg + Ti_2(Cu, Ag)
	8	51.4	48.6							TiAg
	9	12.1	78.5	4				4.4	1	α-Ti + Ti_2(Cu, Ag)
	10		88.9					10.5	0.7	α-Ti
	11		77.2					4.5	18.4	β-Ti
980 °C	1		100							α-Ti
	2	6.0	94.0							α-Ti
	3	20.8	74.6	4.6						Ti_2(Cu, Ag)
	4	6.1	88.3	5.6						α-Ti + Ti_2(Cu, Ag)
	5	30.3	65.7	4.0						TiAg + Ti_2(Cu, Ag)

Independently of the brazing temperatures tested in this investigation, the same phases should constitute the resulting interfaces. The differences were essentially related to the relative amounts of the phases present in each layer, and also in the grain size coarsening of some phases, as the brazing temperature was increased. Layer **1**, after brazing at 900 °C, is composed of a mixture of Ti-rich zones and of Ag-rich particles, which are observed at the central zone of the layer. Attending to the EDS analysis and the Ag-Ti phase diagram, Ti-rich zones should consist of α-Ti, while the central zone of layer **1** should be essentially composed of (Ag). It is also worthy to mention that the formation of oxides such as TiO, TiO_2, and $CuTi_4O$ near ZrO_2 was suggested or confirmed by other authors [7–13]. Oxides presenting a semi-metallic nature, such as TiO and TiO_2, are reported to ensure chemical compatibility and bonding between the ceramic base materials and the interfacial metallic phases. However, the formation of an oxide layer near ZrO_2 could not be clearly confirmed through the SEM/EDS characterization performed in the present study; this may be due in part to the fact that the eventual oxide reaction layer was too thin to be detected by the techniques used in this investigation. Layer **2**, should consist of TiAg (light-grey sub-layer) and Ti_2(Cu, Ag) (grey sub-layer). The central zone of the interface (layer **3**) consists in a mixture of α-Ti + Ti_2(Ag, Cu). Layer **4** present similar microstructural features and composition as those of layer **2**. Layer **5** consists primarily of α-Ti and Ti_2(Ag, Cu) and promotes bonding to the Ti6Al4V alloy. Finally, a diffusion zone was detected, extending up to 50 μm into the base Ti6Al4V alloy, where both the Cu and Ag contents do not exceed 6%.

The characteristic sequence of phases formed at the interface, starting from the ZrO_2 side of the interface, was: Ti oxide(s) + α-Ti (layer **1**)/TiAg + Ti2(Cu, Ni) (layer **2**)/α-Ti + Ti_2(Cu, Ni) (layer **3**)/Ti_2(Cu, Ni) + TiAg (layer **4**)/α-Ti + Ti_2(Cu, Ni) (layer **5**). Figure 6 shows a schematic representation of the evolution of the interfacial microstructure with the brazing temperature. It should be noted that although not depicted in Figure 6, the

formation of a thin oxide layer near ZrO_2, ensuring chemical bonding to either the ceramic sample or the metallic phases that constitute layer 1, should not be discarded.

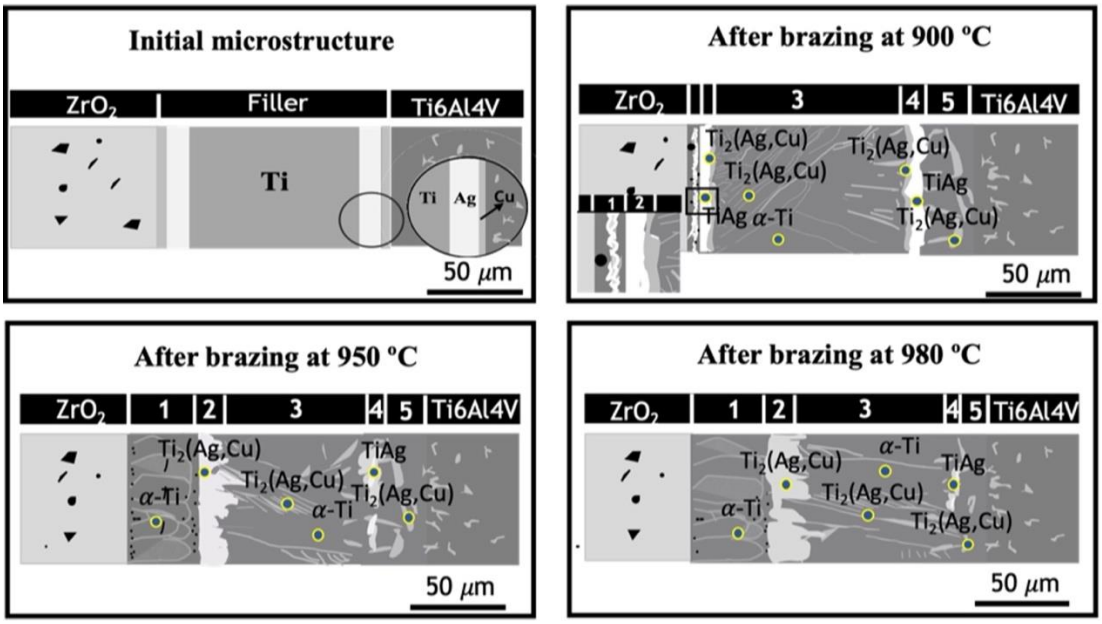

Figure 6. Schematic representation of the evolution of the interfacial microstructure.

The hardness distribution maps of the brazed joints processed at different temperatures are presented in Figure 7. The maps show that the hardness across the interface is relatively uniform and similar to the hardness of Ti6Al4V alloy, with the exception of layer **1**. In fact, the global hardness of layer **1**, which reaches 1715 HV0.01 close to ZrO_2, is significantly higher than the hardness of the remaining interface. These hardness values indicate that layer **1**, in the vicinity of ZrO_2, should be essentially composed of hard phases, instead of just α-Ti and are consistent with the formation of oxide phases reported in other studies. In addition, the hardness distribution maps show that extensive formation of soft phases did not occur, contrarily to the reports in other studies [24–27] where Ag-based fillers were used. This indicates that the novel Ag-Cu sputter-coated Ti brazing filler used in the present investigation potentially avoids the need of eventual post-joining heat treatments to eliminate or minimize the formation of undesirable segregated phases at the interface.

The higher shear strength of joints (152 ± 4 MPa) was obtained after brazing at 980 °C. However, it was not possible to evaluate the shear strength of joints brazed at 950 °C as samples separated as they were being placed in the shear test apparatus. Thus, this processing temperature is inadequate to braze ZrO_2 to Ti6Al4V alloy using Ag-Cu sputter-coated Ti filler. This could be mainly related to the presence of the pores in layer **1**, specifically those observed between the ceramic base material and the interface. In fact, as can be observed in Figure 5, after brazing at 950 °C, the porosity level in layer **1**, near the base ceramic sample, is visibly higher than after processing at either 900 and 980 °C. Indeed, for the two limiting processing temperature used in this study, only residual porosity was observed at this zone of the interface. It should be noted that although brazing at 980 °C induced the formation of pores in layer **1**, these are mainly located near the transition between layer **1** and layer **2**, contrarily to the lower processing temperatures, where pores are mainly located near the ceramic sample. This shifting in the location of most pores, from the hardest zone of layer **1** to a much softer and less brittle zone, appears to be a critical factor impacting the mechanical strength of joints.

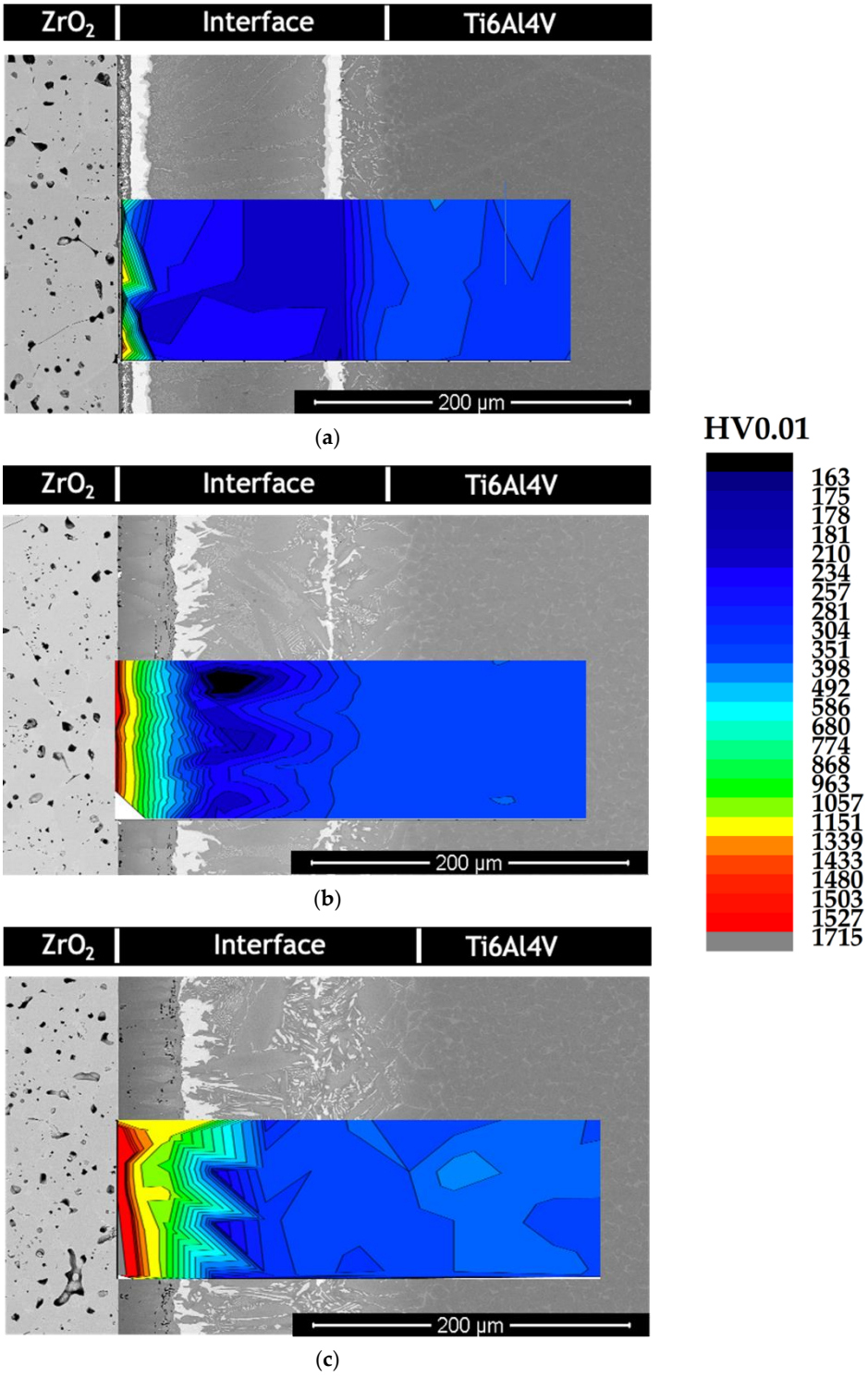

Figure 7. SEM image and hardness distribution maps of the joints processed at (**a**) 900 °C, (**b**) 950 °C, and (**c**) 980 °C.

The lower shear strength of joints (97 ± 2 MPa) after brazing at 900 °C in comparison to brazing at 980 °C, could be related to the combination of two factors. One is related to the already mentioned different porosity distribution features, and the other concerns the formation of a less consolidated/continuous and thinner oxide layer, close to the ZrO_2 sample. Indeed, as the hardness distribution maps presented in Figure 7 denote, the extension of the hardest zone of the interface, which is most likely related to the formation

of oxides phases, increases with the brazing temperature. Thus, after joining at 980 °C, a thicker and possibly more continuous oxide layer, in conjunction with a more favorable porosity distribution in layer **1**, produced the joints displaying the higher shear strength. Figure 8 shows the results of the fracture surface analysis for the samples with the higher shear strength.

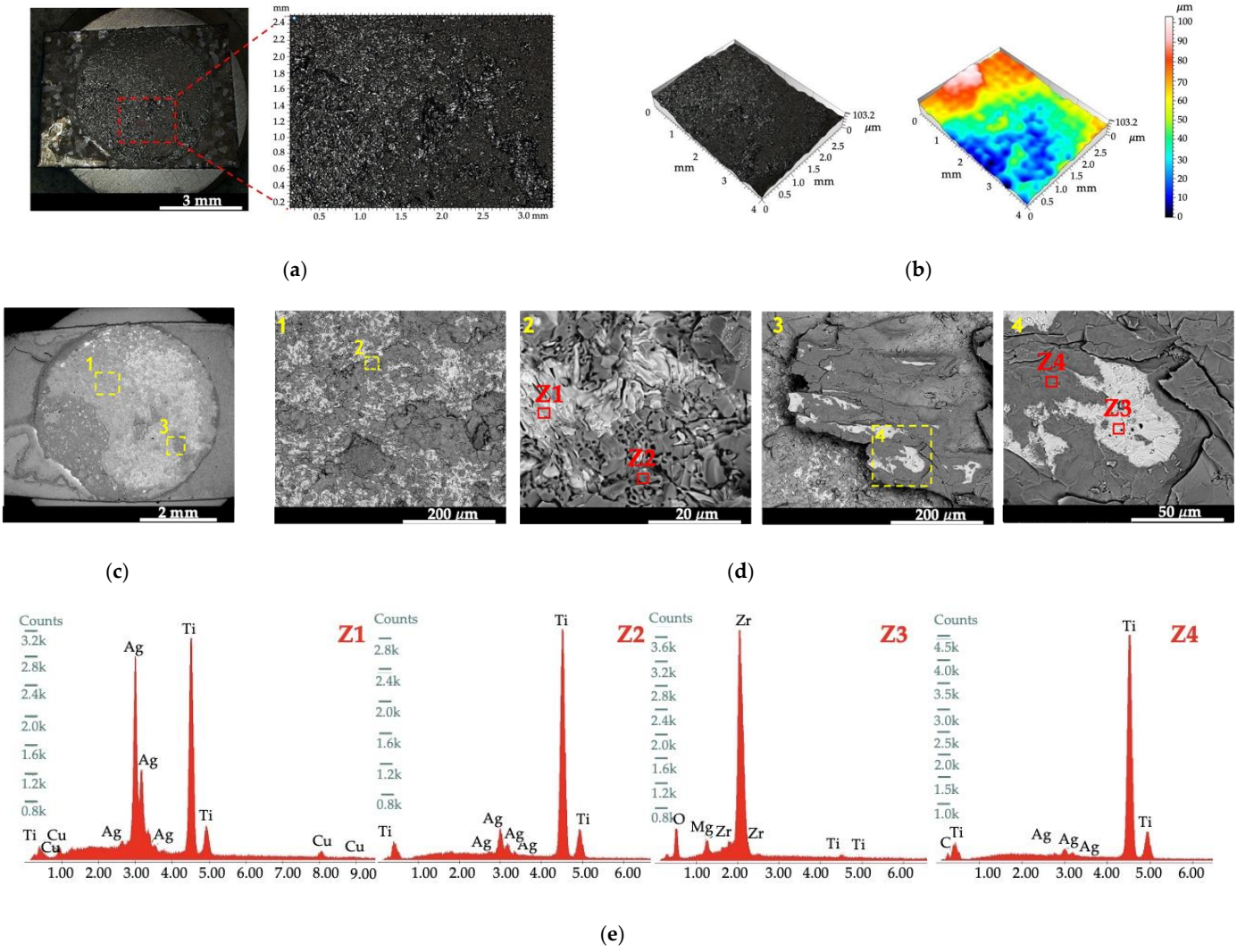

Figure 8. (**a**) Digital microscopy image of the fracture surface on the Ti6Al4V side of joints, (**b**) 3D representation the region marked in (**a**); (**c**) SEM image of the fracture surface and (**d**) magnifications of zones marked in (**c**,**e**) EDS spectra corresponding to the zones marked in (**d**).

Fracture of joints occurred partially across the interface and partially across the ceramic sample. The Ti6Al4V sample was covered by reaction products and with some ceramic fragments still attached to it, while ZrO_2 was partially covered by a visibly thinner layer of reaction products. The SEM/EDS analysis of the fracture surface on the Ti6Al4V alloy side indicates the presence Ti-Ag rich zones, Zr-rich zones and Ti-rich zones. Layer **2** is the only layer, after brazing at 980 °C, which is Ti and Ag rich and, thus, the reactions products labelled as Z1 in Figure 8 should correspond to this layer. The EDS spectra marked as Z2 and Z4 and should correspond to layer **1**, since they correspond to zones essentially composed of Ti with a minor content of Ag. Finally, the ZrO_2 fragments correspond to the spectrum marked as Z3. These results indicate that the fracture of joints occurred partially across the interface, throughout layers **1** and **2**, and partially across the ceramic sample. As can be observed in Figure 9, fracture across the interface occurs essentially at the transition

between layer **1** and layer **2**, where porosity is concentrated, and crack nucleation and propagation are facilitated. Some cracks propagate towards the ceramic sample, across an increasingly harder and brittle layer, eventually penetrating into the ZrO_2 sample, assisting the facture of the joints.

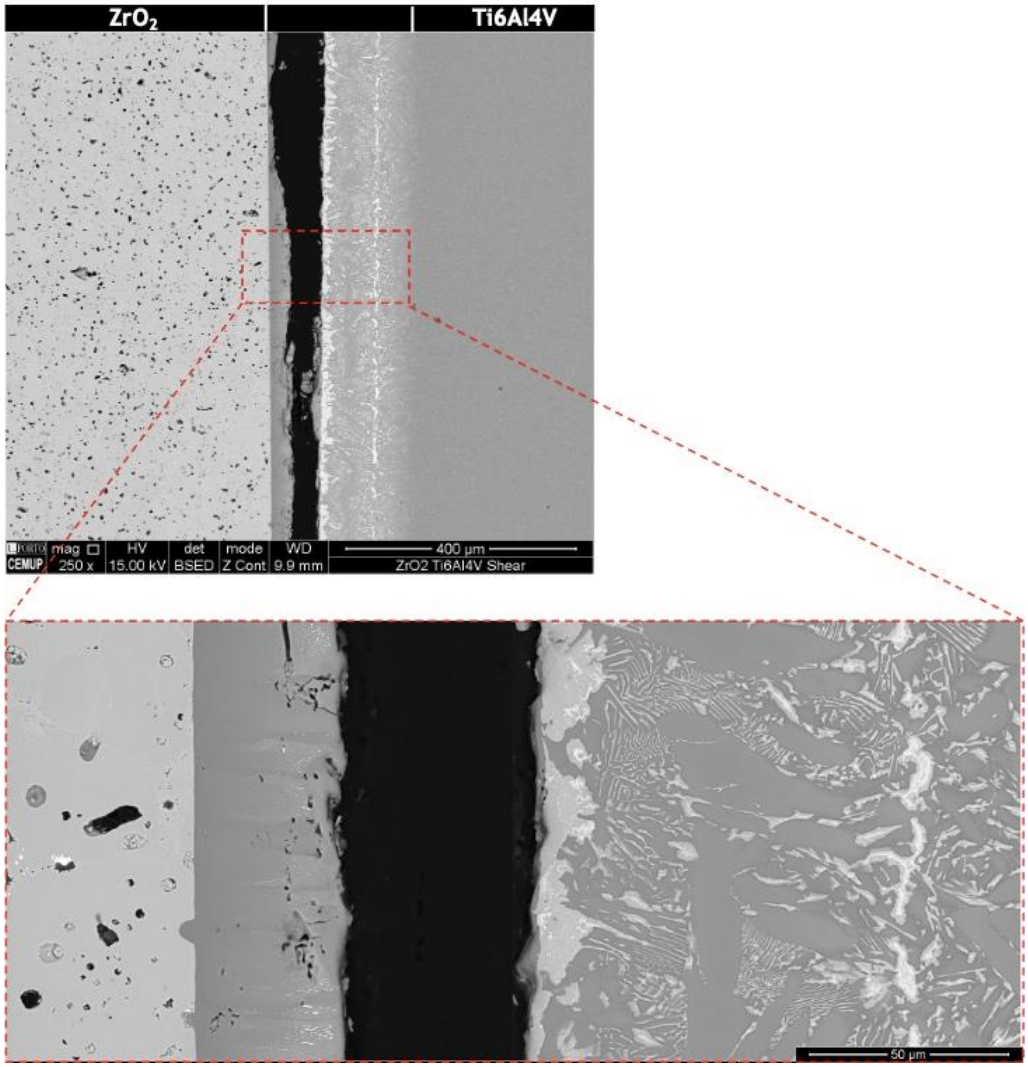

Figure 9. SEM image of the cross-section of the interface of fractured joints, processed at 980 °C after shear testing.

4. Conclusions

The joining of ZrO_2 to Ti6Al4V alloy was investigated, using Ag-Cu sputter-coated Ti foil as a brazing filler. Brazing was carried out in a vacuum at 900, 950 and 980 °C for 30 min.

The typical multilayered microstructure of the interface could be described as: base Zirconia (ZrO_2 + MgO)/layer 1: Ti oxide(s) + α-Ti/layer 2: TiAg + Ti_2(Cu, Ni)/layer 3: α-Ti + Ti_2(Cu, Ni)/layer 4: Ti_2(Cu, Ni) + TiAg/layer 5: α-Ti + Ti_2(Cu, Ni)/base Ti6Al4V (α-Ti + β-Ti).

The hardness throughout the interfaces is relatively homogeneous and similar to the hardness of Ti6Al4V, with the exception of the Ti-rich layer formed near ZrO_2. This layer is the hardest region of the interface and exhibits a steep declining hardness gradient, with a maximum hardness of c.a. 1715 HV0.01 close to ZrO_2.

The highest shear strength (152 ± 4 MPa) was displayed for joints processed at 980 °C. Fracture of joints occurred partially across the interface, throughout the layers formed near ZrO_2 and partially across the ceramic sample.

The results obtained in this investigation also indicate that the use of Ag-Cu sputter-coated Ti foil as a brazing filler for joining ZrO_2 to Ti6Al4V, potentially avoids the need of eventual post-joining heat treatments to eliminate or minimize the formation of undesirable segregated phases at the interface.

Author Contributions: Conceptualization, A.G., C.J.T. and S.S.; methodology, O.E.; validation, A.G., C.J.T. and S.S.; formal analysis, O.E., A.G. and S.S.; investigation, O.E. and S.S.; resources, S.S.; writing—original draft preparation, S.S.; writing—review and editing, A.G., C.J.T. and S.S.; visualization, O.E. and S.S.; supervision, A.G. and S.S.; project administration, S.S.; funding acquisition, S.S. All authors have read and agreed to the published version of the manuscript.

Funding: This work was financially supported by: Project PTDC/CTM-CTM/31579/2017—POCI-01-0145-FEDER-031579-funded by FEDER funds through COMPETE2020—Programa Operacional Competitividade e Internacionalização (POCI) and by national funds (PIDDAC) through FCT/MCTES.

Institutional Review Board Statement: Not applicable.

Informed Consent Statement: Not applicable.

Data Availability Statement: Data can be available upon request from the authors.

Acknowledgments: The authors also acknowledge the CEMUP (Centro de Materiais da Universidade do Porto) for microscopy assistance.

Conflicts of Interest: The authors declare no conflict of interest.

References

1. Leyens, C.; Peters, M. (Eds.) *Titanium and Titanium Alloys*; Wiley: New York, NY, USA, 2003; ISBN 9783527305346.
2. Carter, C.B.; Norton, M.G. *Ceramic Materials*; Springer: New York, NY, USA, 2007; ISBN 978-0-387-46270-7.
3. Richerson, D.W.; Lee, W.E. *Modern Ceramic Engineering: Properties, Processing, and Use in Design*, 4th ed.; Taylor & Francis Group: Boca Raton, FL, USA, 2018.
4. Uday, M.B.; Ahmad-Fauzi, M.N.; Alias, M.N.; Srithar, R. Current Issues and Problems in the Joining of Ceramic to Metal. In *Joining Technologies*; Ishak, M., Ed.; IntechOpen: London, UK, 2016; pp. 159–193.
5. Dai, X.; Cao, J.; Liu, J.; Wang, D.; Feng, J. Interfacial reaction behavior and mechanical characterization of ZrO_2/TC4 joint brazed by Ag-Cu filler metal. *Mater. Sci. Eng. A* **2015**, *646*, 182–189. [CrossRef]
6. Li, H.; Liu, H.; Huang, H. Microstructure and properties of ZrO_2 ceramic and Ti-6Al4V alloy vacuum brazed by Ti-28Ni filler metal. *Weld. Technol. Rev.* **2019**, *91*, 35–41. [CrossRef]
7. Dai, X.; Cao, J.; Wang, Z.; Wang, X.; Chen, L.; Huang, Y.; Feng, J. Brazing ZrO_2 ceramic and TC4 alloy by novel WB reinforced Ag-Cu composite filler: Microstructure and properties. *Ceram. Int.* **2017**, *43*, 15296–15305. [CrossRef]
8. Liu, Y.; Hu, J.; Zhang, Y.; Guo, Z.; Yang, Y. Joining of zirconia and Ti-6Al-4V using a Ti-based amorphous filler. *J. Mater. Sci. Technol.* **2011**, *27*, 653–658. [CrossRef]
9. Liu, Y.; Hu, J.; Zhang, Y.; Guo, Z. Interface microstructure of the brazed zirconia and Ti-6Al-4V using Ti-based amorphous filler. *Sci. Sinter.* **2013**, *45*, 313–321. [CrossRef]
10. Liu, Y.; Hu, J.; Shen, P.; Guo, Z.; Liu, H. Effect of fabrication parameters on interface of zirconia and Ti-6Al-4V joints using Zr55Cu30Al10Ni5 amorphous filler. *J. Mater. Eng. Perform.* **2013**, *22*, 2602–2609. [CrossRef]
11. Liu, Y.H.; Hu, J.D.; Shen, P.; Han, X.H.; Li, J.C. Microstructural and mechanical properties of jointed ZrO_2/Ti-6Al-4V alloy using $Ti_{33}Zr_{17}Cu_{50}$ amorphous brazing filler. *Mater. Des.* **2013**, *47*, 281. [CrossRef]
12. Cao, J.; Song, X.G.; Li, C.; Zhao, L.Y.; Feng, J.C. Brazing ZrO_2 ceramic to Ti-6Al-4V alloy using NiCrSiB amorphous filler foil: Interfacial microstructure and joint properties. *Mater. Charact.* **2013**, *81*, 85–91. [CrossRef]
13. Liang, Y.; Kong, J.; Dong, K.; Song, X.; Liu, X.; Zhu, R. Microstructure evolution and mechanical properties of vacuum brazed ZrO_2/Ti-6Al-4V joint utilizing a low-meting-point amorphous filler metal. *Vacuum* **2021**, *192*, 110156. [CrossRef]
14. Hardesty, R.; Jensen, M.; Grant, L. *High Temperature Be Panel Development*; NASA Contract Report 181777; NASA: Hampton, VA, USA, 1989.
15. Emadinia, O.; Guedes, A.; Tavares, C.J.; Simões, S. Joining alumina to titanium alloys using Ag-Cu sputter-coated Ti brazing filler. *Materials* **2020**, *13*, 4802. [CrossRef] [PubMed]
16. Simões, S.; Tavares, C.J.; Guedes, A. Joining of TiAl Alloy to Ni-Based Superalloy Using Ag-Cu Sputtered Coated Ti Brazing Filler Foil. *Metals* **2018**, *8*, 723. [CrossRef]

17. Simões, S.; Soares, A.; Tavares, C.J.; Guedes, A. Joining of TiAl Alloy Using Novel Ag-Cu Sputtered Coated Ti Brazing Filler. *Microsc. Microanal.* **2019**, *25*, 192–195. [CrossRef] [PubMed]
18. Okamoto, H.; Schlesinger, M.E.; Mueller, E.M. *ASM Handbook: Alloy Phase Diagrams*; ASM International: Almere, The Netherlands, 2016; Volume 3.
19. Villars, P.; Prince, A.; Okamoto, H. *Handbook of Ternary Alloy Phase Diagrams*; ASM International: Almere, The Netherland, 1995.
20. Lukas, H.L. Ag-Al-Ti (Silver-Aluminium-Titanium) in Landolt-Bornstein New Series G. In *Light Metal Ternary Systems: Phase Diagrams, Crystallographic and Thermodynamic Data: Light Metal Systems*; Part 1; Effenberg, G., Ilyenko, S., Eds.; Springer: New York, NY, USA, 2004; Volume 11A1.
21. Ahmed, T.; Flower, H.M. Partial isothermal sections of Ti–Al–V ternary diagram. *Mater. Sci. Technol.* **1994**, *10*, 272–288. [CrossRef]
22. Raghavan, V. Al-Nb-Ti (Aluminum-Niobium-Titanium). *J. Phase Equilibria Diffus.* **2010**, *31*, 47–52. [CrossRef]
23. Schmid-Fetzer, R. Al-Cu-Ti (Aluminium-Copper-Titanium) in Landolt-Bornstein New Series G. In *Light Metal Ternary Systems: Phase Diagrams, Crystallographic and Thermodynamic Data: Light Metal Systems*; Part 2; Effenberg, G., Ilyenko, S., Eds.; Springer: New York, NY, USA, 2005; Volume 11A2.
24. Cao, J.; Zheng, Z.J.; Wu, L.Z.; Qi, J.L.; Wang, Z.P.; Feng, J.C. Processing, microstructure and mechanical properties of vacuum-brazed Al_2O_3/Ti6Al4V joints. *Mater. Sci. Eng. A* **2012**, *535*, 62–67. [CrossRef]
25. Niu, G.B.; Wang, D.P.; Yang, Z.W.; Wang, Y. Microstructure and mechanical properties of Al_2O_3 ceramic and TiAl alloy joints brazed with Ag-Cu-Ti filler metal. *Ceram. Int.* **2016**, *42*, 6924–6934. [CrossRef]
26. Yang, Z.; Lin, J.; Wang, Y.; Wang, D. Characterization of microstructure and mechanical properties of Al_2O_3/TiAl joints vacuum-brazed with Ag-Cu-Ti + W composite filler. *Vacuum* **2017**, *143*, 294–302. [CrossRef]
27. Liu, X.; Zhang, L.; Sun, Z.; Feng, J. Microstructure and mechanical properties of transparent alumina and TiAl alloy joints brazed using Ag-Cu-Ti filler metal. *Vacuum* **2018**, *151*, 80–89. [CrossRef]